

Analytical theory and possible detection of the ac quantum spin Hall effect

W. Y. Deng¹, Y. J. Ren¹, Z. X. Lin¹, L. Sheng^{1,2,*}, D. N. Sheng³, and D. Y. Xing^{1,2}

¹ National Laboratory of Solid State Microstructures and Department of Physics, Nanjing University, Nanjing 210093, China

² Collaborative Innovation Center of Advanced Microstructures, Nanjing University, Nanjing 210093, China

³ Department of Physics and Astronomy, California State University, Northridge, California 91330, USA

(Dated: May 18, 2021)

We develop an analytical theory of the low-frequency ac quantum spin Hall (QSH) effect based upon the scattering matrix formalism. It is shown that the ac QSH effect can be interpreted as a bulk quantum pumping effect. When the electron spin is conserved, the integer-quantized ac spin Hall conductivity can be linked to the winding numbers of the reflection matrices in the electrodes, which also equal to the bulk spin Chern numbers of the QSH material. Furthermore, a possible experimental scheme by using ferromagnetic metals as electrodes is proposed to detect the topological ac spin current by electrical means.

PACS numbers: 72.25.-b, 73.43.-f, 73.23.-b, 75.76.+j

I. INTRODUCTION

Topological insulators (TIs) are currently on the research front of condensed matter physics, because of their fundamental interest and potential applications in spintronic devices [1–13]. Two-dimensional (2D) TIs are also called the quantum spin Hall (QSH) systems, as they can host the interesting QSH effect, in which quantized spin current or spin accumulation can be generated in response to an applied electric field. A QSH system is an insulator in the bulk with a pair of conducting gapless edge states traversing the bulk band gap [1–3]. The existence of the edge states has its origin in the nontrivial bulk topological properties, which are usually characterized by the Z_2 index [14] or spin Chern numbers [15–17], but their gapless nature is protected by the time-reversal (TR) symmetry. While the nondissipative electronic transport through the edge modes is immune to nonmagnetic disorder, the edge states will become gapped and Anderson localized in the presence of TR-symmetry-breaking perturbations [1, 18]. As a consequence, the QSH effect is often unstable in realistic environments. Up to now, conductance through edge channels near the theoretically predicted quantized value has been detected only in small samples of HgTe quantum wells [19] and InAs/GaSb bilayers [20]. Realizing QSH effect that is as robust as the conventional quantum Hall effect is still challenging.

Recently, it was numerically demonstrated that the ac QSH effect driven by an ac electric field is fundamentally different from the intensively researched dc QSH effect [21]. In contrast to the dc QSH effect, which must be carried by edge states, the ac QSH effect can occur in the bulk without involving the fragile edge states, hence being robust against TR-symmetry breaking and disorder. In fact, ac spin-dependent electronic transport has started to capture attention in recent years, stimulat-

ing the emerging field of ac spintronics. Jiao and Bauer theoretically predicted that the much larger ac voltage could be used to detect spin currents in the spin pumping transport [22]. Wei *et al.* found experimentally that the ac spin current is much larger than the dc component in a ferromagnet-normal junction with time-dependent magnetization vector [23].

In this paper, we show that the basic characteristics of the low-frequency ac QSH effect can be described by a simple analytical theory based on the time-dependent scattering matrix formalism. The ac spin Hall conductivity in the adiabatic regime is linked to the winding numbers of the reflection matrices in the electrodes, which also equal to the spin Chern numbers of the QSH material. The theoretical result is consistent with the numerical calculation based upon the Kubo linear-response theory [21]. Our theory indicates that while the ac and dc QSH effects behave quite differently, they share the same topological origin. We further show that when ferromagnetic metals are used as electrodes, the topological ac spin current will induce an electrical voltage difference along the electrodes, suggesting a possible experimental way to observe the ac QSH effect by electrical means.

In the next section, we present a general theoretical description of the ac QSH effect based on the scattering matrix formula. In Sec. III, we consider the BHZ model as a concrete example, and evaluate the winding numbers and spin Hall conductivity. In Sec. IV, a possible way to measure the ac spin Hall conductivity experimentally is proposed. The final section contains a summary.

II. A GENERAL DESCRIPTION

Let us consider the setup illustrated in Fig. 1. Two metallic bars (blue) are deposited on top of a QSH sample. When an ac electric voltage difference is applied to the bars, an ac electric field $E(t) = E_0 \cos(\omega t)$ is established between the bars, and in response, a Hall spin current $j_s(t)$ is generated in the biased region. Two metallic

*Electronic address: shengli@nju.edu.cn

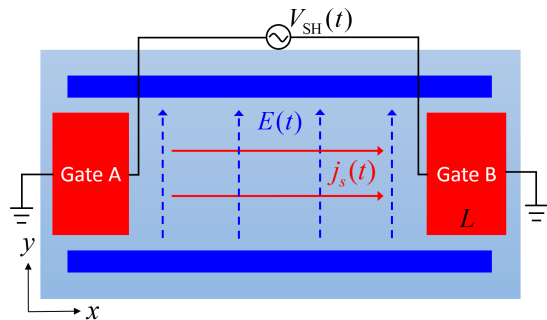


FIG. 1: A schematic view of a proposed setup to study the topological *ac* QSH effect. Two metal bars (blue) are deposited on top of a 2D QSH material. When an *ac* electrical voltage is applied to the metal bars, an electric field $E(t)$ will be generated in the y direction. In response, an *ac* Hall spin current $j_s(t)$ is created along the x direction. Two metal gates (red) with length L , i.e., gates A and B , are deposited near the two edges of the biased region as source and drain electrodes for the spin current. We first assume the electrodes to be nonmagnetic. Later, we will show that if ferromagnetic metals are used as the electrodes, an *ac* electric voltage difference $V_{\text{SH}}(t)$ can be induced between the inside edges of the two electrodes, suggesting a possible way to detect the *ac* QSH effect electrically.

gates (red), A and B , are deposited between the bars near the edges of the biased region, which serve as source and drain electrodes for the Hall spin current. To facilitate our general discussion, we assume that the *ac* electric field also exists in the electrodes. This assumption does not change the topological properties of the system, and will not affect the main conclusion. The sizes of the biased region and electrodes are taken to be sufficiently large, so that we can neglect any finite-size effects. As a result, the Hamiltonian of the system of the biased region and electrodes takes the form $H(k_x, \tilde{k}_y, x)$ with $\tilde{k}_y = k_y - eA(t)$. Here, (k_x, k_y) is the 2D momentum, where $k_x = \frac{\hbar}{i} \frac{\partial}{\partial x}$ is an operator, and k_y is a good quantum number. $A(t) = -\frac{E_0}{\omega} \sin(\omega t)$ is the vector potential of the *ac* electric field $\vec{E}(t) = E_0 \cos(\omega t)$. In the biased region, $H(k_x, \tilde{k}_y, x)$ is the Hamiltonian of the QSH material with a band gap, while in the electrodes, it represents the Hamiltonian of a metal. The remaining region of the QSH sample, which is neither excited by the *ac* electric field nor in contact with the electrodes, will behave just like an ordinary insulator [21], and so is not included into the Hamiltonian.

The electron Fermi energy is set to be in the band gap of the QSH material. We consider first the ideal case, where the electron spin is conserved. We focus on the right electrode, and the situation in the left electrode is similar. Let $\hat{r}_{ss}(\tilde{k}_y)$ be the reflection matrix for an electron with spin s (\uparrow or \downarrow) at the Fermi level transmitting from the electrode toward the biased region. In the adiabatic regime, the spin current density pumped into the electrode at time t can be evaluated by using the scat-

tering matrix formula [24, 25]

$$j_s(t) = \frac{1}{L_y} \left(\frac{\hbar}{4\pi i} \right) \sum_{k_y \in \text{BZ}} \text{Tr} \left(\hat{r}_{\uparrow\uparrow}^\dagger \frac{d}{dt} \hat{r}_{\uparrow\uparrow} - \hat{r}_{\downarrow\downarrow}^\dagger \frac{d}{dt} \hat{r}_{\downarrow\downarrow} \right), \quad (1)$$

with L_y as the cross-section of the biased region. We notice that the reflection matrices depend on t only through the variable $\tilde{k}_y = k_y - eA(t)$, such that $\frac{d}{dt} \hat{r}_{\uparrow\uparrow} = eE(t) \frac{d}{dk_y} \hat{r}_{\uparrow\uparrow}$, and $\frac{d}{dt} \hat{r}_{\downarrow\downarrow} = eE(t) \frac{d}{dk_y} \hat{r}_{\downarrow\downarrow}$. By using these relations and replacing the summation over k_y in Eq. (1) by an integral, we derive the *ac* spin Hall conductivity, defined as $\sigma_{\text{SH}}(\omega) = j_s(t)/E(t)$, to be

$$\sigma_{\text{SH}}(\omega) = \frac{e}{4\pi} (W_\uparrow - W_\downarrow), \quad (2)$$

where

$$W_s = \frac{1}{2\pi i} \int_{\text{BZ}} dk_y \text{Tr} \left(\hat{r}_{ss}^\dagger \frac{d}{dk_y} \hat{r}_{ss} \right). \quad (3)$$

Since the electron Fermi energy is in the band gap of the QSH material, an electron incident from the electrode will be fully reflected, and the reflection matrices must be unitary, i.e., $\hat{r}_{ss}^\dagger(\tilde{k}_y) \hat{r}_{ss}(\tilde{k}_y) = \hat{1}$. Besides, they are periodic functions of k_y in a Brillouin zone. As a result, one can identify immediately W_s as winding numbers, which are always integers. Therefore, while the spin Hall conductivity $\sigma_{\text{SH}}(\omega)$ is defined as the ratio between two time-dependent quantities, i.e., the *ac* spin current $j_s(t)$ and *ac* electric field $E(t)$, it is integer-quantized at any time, in units of the spin conductivity quantum $\frac{e}{4\pi}$, in the adiabatic regime. Very often, continuous models are employed in theoretical works. In a well-defined continuous model, the electron wavefunctions should be continuous in the $k_y \rightarrow \pm\infty$ limit, which implies

$$\lim_{k_y \rightarrow +\infty} \hat{r}_{ss}(\tilde{k}_y) = \lim_{k_y \rightarrow -\infty} \hat{r}_{ss}(\tilde{k}_y). \quad (4)$$

Under this condition, W_s remain to be integer-quantized. In the example considered later, we will see that W_s in fact equal to the spin Chern numbers of the QSH system. When small spin-mixing perturbations, such as the Rashba spin-orbit coupling, are present, spin-flip reflection processes will occur with small probabilities, and the *ac* spin Hall conductivity will deviate from the integer-quantized value in a gradual manner, similarly to the *dc* QSH effect.

We need to point out that the *ac* Hall spin current originates from the time dependence of the Hamiltonian caused by the *ac* applied electric field, as clearly indicated by Eq. (1). One might think that by taking the limit $\omega \rightarrow 0$, the conclusion for the *ac* QSH effect should be applicable to the *dc* QSH effect, which is not true. For an exactly static electric field ($\omega = 0$), since one can choose an electrostatic scalar potential to make the Hamiltonian independent of time, no spin current can be generated in the setup shown in Fig. 1. The *dc* QSH effect must be carried by the edge states. Therefore, the *ac*

QSH effect is substantially different from the *dc* QSH effect. Moreover, the above general discussion about the *ac* QSH effect does not rely on any symmetries, which is also different from the *dc* QSH effect. Small TR-symmetry-breaking perturbations will open an energy gap in the spectrum of the edge states in a QSH material, and the edge states become exponentially localized immediately due to their one-dimensional nature. As a consequence, the *dc* QSH effect will be destroyed for sufficiently large samples. In contrast, the *ac* QSH effect is a bulk transport phenomenon, being robust against TR-symmetry breaking and disorder [21].

III. A CONCRETE EXAMPLE

As a concrete example, we consider the BHZ model, which can be used to describe the HgTe quantum wells [26] or InAs/GaSb bilayers [27]. The BHZ model Hamiltonian reads

$$H_{\text{QSH}} = v_{\text{F}}(k_x \hat{s}_z \hat{\sigma}_x - \tilde{k}_y \hat{\sigma}_y) - (M_0 - B\tilde{k}^2) \hat{\sigma}_z. \quad (5)$$

Here, we retain the $B\tilde{k}^2$ term with $\tilde{k}^2 = k_x^2 + \tilde{k}_y^2$, as it ensures that the condition Eq. (4) is fulfilled, and the topological properties of the system are properly defined. In fact, the spin Chern numbers of this model, given by $C_{\uparrow(\downarrow)} = \pm \frac{1}{2}[\text{sgn}(M_0) + \text{sgn}(B)]$ [28], are dependent of B . Other nonessential nonlinear terms of momentum in the original model have been neglected for simplicity.

The *ac* QSH effect, as a topological transport phenomenon, is insensitive to the material details of the electrodes. We model the electrodes by using a simple parabolic Hamiltonian $H_{\text{E}} = -U_0 + \frac{\tilde{k}^2}{2m}$. U_0 is taken to be large compared with all other energy scales, so as to guarantee that the electrodes have sufficient number of conducting channels for the spin current to flow through. Finite potential barriers of height V_0 and thickness d exist at the interfaces between the QSH material and electrodes, similar to the setup considered in Ref. [29]. By following the same procedure detailed in Ref. [29], linearizing the Hamiltonians of both the QSH material and electrodes with respect to k_x , one can obtain for the reflection coefficients

$$r_{\uparrow\uparrow}(\tilde{k}_y) = -\frac{\cos(\theta) + i[\text{sh}(\gamma_0 d) - \sin(\theta)\text{ch}(\gamma_0 d)]}{\text{ch}(\gamma_0 d) - \sin(\theta)\text{sh}(\gamma_0 d)}, \quad (6)$$

and $r_{\downarrow\downarrow}(\tilde{k}_y) = r_{\uparrow\uparrow}(\tilde{k}_y)|_{\theta \rightarrow (\pi - \theta)}$, where $\gamma_0 = \frac{V_0}{\hbar} \sqrt{2m/U_0}$ and $\theta = \arg[v_{\text{F}} \tilde{k}_y + i(M_0 - B\tilde{k}_y^2)]$.

For the present model, the reflection matrix $\hat{r}_{ss}(\tilde{k}_y)$ is simply a number, satisfying $|r_{ss}|^2 = 1$. Therefore, with changing k_y from $-\infty$ to ∞ , $r_{ss}(\tilde{k}_y)$ keeps traveling on the unit circle around the origin on the complex plane, and forms a closed orbit due to single-value condition Eq. (4). The quantity W_s defined in Eq. (3) is the winding number of the closed orbit around the origin. For

convenience, the winding number may also be expressed as

$$W_s = \frac{1}{2\pi} [\varphi_s(\infty) - \varphi_s(-\infty)], \quad (7)$$

where $\varphi_s(k_y)$ is the argument of $r_{ss}(\tilde{k}_y)$. In the absence of the potential barrier, i.e., $\gamma_0 d = 0$, the reflection amplitude Eq. (6) reduces to $r_{\uparrow\uparrow}(k_y) = -e^{-i\theta}$. The winding number can be determined by tracking how the argument $\varphi_s(k_y)$ of $r_{ss}(\tilde{k}_y)$ evolves with changing k_y from $-\infty$ to ∞ . In Fig. 2(a), we plot four different representative behaviors of $\varphi_{\uparrow}(k_y)$. For simplicity, we have chosen the unit set, where $v_{\text{F}} = |M_0| = 1$. From Fig. 2(a), we see that if $M_0 > 0$ and $B > 0$, $\varphi_{\uparrow}(k_y)$ increments 2π with varying k_y from $-\infty$ to ∞ . If $M_0 < 0$ and $B < 0$, $\varphi_{\uparrow}(k_y)$ decrements 2π . In the other cases, where $M_0 > 0$ and $B < 0$, or $M_0 < 0$ and $B > 0$, $\varphi_{\uparrow}(k_y)$ does not change. The behaviors of $\varphi_{\downarrow}(k_y)$ can be analyzed similarly. Consequently, we obtain from Eq. (7) the following expression for the winding numbers

$$W_{\uparrow(\downarrow)} = \pm \frac{1}{2} [\text{sgn}(M_0) + \text{sgn}(B)] \equiv C_{\uparrow(\downarrow)}. \quad (8)$$

Interestingly, the winding numbers are exactly equal to the spin Chern numbers of the BHZ model. As expected, the *ac* spin Hall conductivity is integer-quantized, $\sigma_{\text{SH}} = [\text{sgn}(M_0) + \text{sgn}(B)] \frac{e}{4\pi} \equiv (C_{\uparrow} - C_{\downarrow}) \frac{e}{4\pi}$, which is consistent with the numerical result calculated from the Kubo theory at low frequencies [21]. This relation indicates that while the *ac* and *dc* QSH effects behave quite differently, they share the same topological origin.

For a nonvanishing potential barrier, i.e., $\gamma_0 d > 0$, the condition $|r_{ss}|^2 = 1$ is still satisfied. This means that with changing k_y from $-\infty$ to ∞ , the reflection amplitudes $r_{ss}(\tilde{k}_y)$ always move on the unit circle around the origin on the complex plane. As a result, the winding numbers cannot change values with changing $\gamma_0 d$. In other words, Eq. (8) remains valid for a nonvanishing potential barrier. Here, based upon the same topological argument, we may also get some insight into why the *ac* spin Hall conductivity $\sigma_{\text{SH}}(\omega) = j_s(t)/E(t)$ is integer-quantized, being independent of time. At a given time t , the system Hamiltonian $H(t)$ has some small deformation from $H(t=0)$. As long as the difference $H(t) - H(0)$ is not large enough to close the band gap, the winding numbers and spin Hall conductivity are unchangeable. In Fig. 2(b), we plot the argument $\varphi_{\uparrow}(k_y)$ of $r_{\uparrow\uparrow}(k_y)$ for some different sets of $\gamma_0 d$ and ωt in the case $M_0 > 0$ and $B > 0$. We see that while its curve deforms with changing $\gamma_0 d$ or ωt , $\varphi_{\uparrow}(k_y)$ always increments 2π , independent of the barrier strength or time. For essentially the same reason, it is easy to understand that whether the *ac* electric field exists in the electrode does not affect the expressions for the winding numbers and *ac* spin Hall conductivity. The winding numbers may change values, only if the bulk band gap in the QSH material closes. In this case, the condition $|r_{ss}|^2 = 1$ of full reflection no longer holds, and the trajectories of $r_{ss}(\tilde{k}_y)$ can sweep

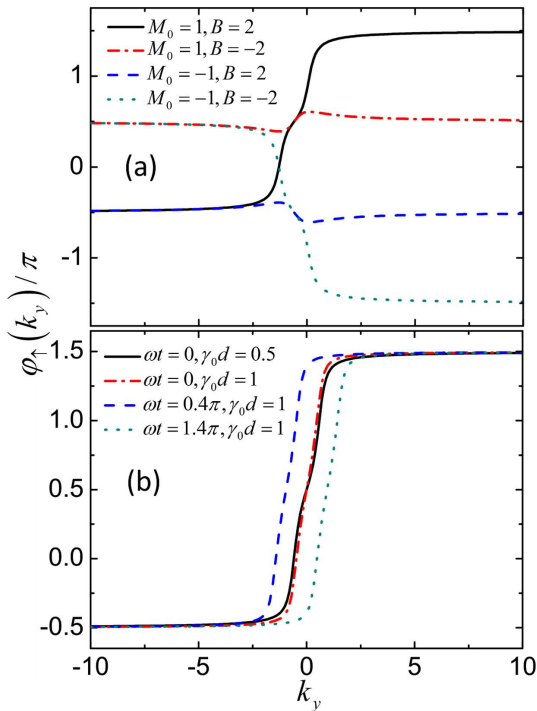


FIG. 2: Argument of the complex reflection amplitude, $\varphi_{\uparrow}(k_y) = \arg(r_{\uparrow\uparrow})$, as a function of k_y , for (a) four different sets of (M_0, B) , and (b) four sets of $(\omega t, \gamma_0 d)$. The other parameters are taken to be $eE_0/\omega = 1$, and (a) $\omega t = \gamma_0 d = 0$, (b) $M_0 = 1, B = 2$.

across the origin on the complex plane, which leads to a change in the winding numbers, signaling a topological phase transition.

Similarly to Ref. [29], one can also include the Rashba spin-orbit coupling into H_{QSH} , and find that it leads to small deviation of the spin Hall conductivity from the integer-quantized value, in the second order of R/v_F with R as the strength of the Rashba spin-orbit coupling.

IV. EXPERIMENTAL MEASUREMENT OF THE AC QSH EFFECT

Now we propose a method to experimentally measure the *ac* spin Hall conductivity by electrical means. For the same setup shown in Fig. 1, we suggest to use ferromagnetic metals as gates *A* and *B*, with their magnetic moments aligned along the *z* axis. The ferromagnets are assumed to have a length L , in the *x* direction, much greater than the spin diffusion length ℓ_D . As demonstrated above, the spin current generated is topological and insensitive to the material parameters of the electrodes. When the *ac* electric field $E(t)$ is applied, a pure *ac* spin current density $\sigma_{\text{SH}}E(t)$ will flow out of the source electrode and into the drain electrode. The principle of the proposed method can be explained as follows. The amplitude of the spin current decays into the elec-

trodes within about a spin diffusion length ℓ_D , and its spin-up and spin-down components recombine to cancel each other. Since the majority-spin and minority-spin bands of a ferromagnet have different 2D conductivities, σ_M and σ_m , the voltage drops (strictly speaking, drops of the electrochemical potential) in the two spin channels caused by the spin current are not equal in magnitudes, giving rise to a net *ac* electric voltage drop. If the voltages at the outside edges of the ferromagnetic electrodes are made equal through grounding or short-circuiting, as shown in Fig. 1, a voltage difference $V_{\text{SH}}(t)$ will appear between the inner edges of the electrodes, which can be measured by using an *ac* voltage meter.

To calculate the voltage difference, we employ the semiclassical spin diffusion equation for a ferromagnetic metal, which can be written as [30]

$$\nabla^2 \mu_s(x, t) = \frac{\mu_s(x, t) - \mu_{-s}(x, t)}{l_s^2}. \quad (9)$$

Here, $l_s = v_F \sqrt{\tau_s \tau_{\uparrow\downarrow}/3}$, where τ_s and $\tau_{\uparrow\downarrow}$ are the electron non-spin-flip and spin-flip relaxation times, $\mu_s(x, t)$ is the spin-dependent electrochemical potential for spin-up ($s = \uparrow$) and spin-down ($s = \downarrow$) electrons, respectively, and v_F is the Fermi velocity in the ferromagnets. The usually small spin dependence in the Fermi velocity has been neglected [31, 32]. The spin-dependent electrical current is given by

$$\mathcal{J}_s(x, t) = -\sigma_s \nabla \mu_s(x, t), \quad (10)$$

where $\sigma_s = e^2 \tau_s k_F^3 / 6\pi^2 m$ is the Drude conductivity.

We consider first the drain electrode *B*. In this case, the topological pure spin current $\sigma_{\text{SH}}E(t)$ flows from the QSH material into the electrode. The boundary condition at the left edge ($x = 0$) of the electrode is given by

$$\mathcal{J}_{\uparrow}(0, t) = -\mathcal{J}_{\downarrow}(0, t) = \frac{e}{\hbar} \sigma_{\text{SH}} E(t), \quad (11)$$

while that at the right edge ($x = L$) reads

$$\mu_{\uparrow}(L, t) = \mu_{\downarrow}(L, t) = 0, \quad (12)$$

since the right edge is grounded. From Eqs. (9)-(12), one can readily obtain for the spin-dependent electrochemical potential

$$\mu_{\uparrow}(x, t) = -\mu_0 \frac{\ell_D^2}{l_{\uparrow}^2} e^{-x/\ell_D}, \quad (13)$$

$$\mu_{\downarrow}(x, t) = \mu_0 \frac{\ell_D^2}{l_{\downarrow}^2} e^{-x/\ell_D}, \quad (14)$$

with

$$\mu_0(t) = \frac{e}{\hbar} \sigma_{\text{SH}} E(t) \ell_D \left(\frac{1}{\sigma_{\uparrow}} + \frac{1}{\sigma_{\downarrow}} \right),$$

where $\ell_D^{-2} = l_{\uparrow}^{-2} + l_{\downarrow}^{-2}$ and ℓ_D is the spin-diffusion length. The electric voltage $\mu(x, t)$ in the ferromagnet is the average of spin up and down chemical potentials, $\mu(x, t) = \frac{1}{2} [\mu_{\uparrow}(x, t) + \mu_{\downarrow}(x, t)]$.

The electric voltage in gate A can be solved similarly. We find that the electric voltage at the right edge of gate A is equal to that at the left edge of gate B in magnitude, but with an opposite sign. As a result, the electric voltage difference between the two inside edges of gates A and B is $V_{\text{SH}}(t) = 2\mu(0, t)$, which can be derived to be

$$V_{\text{SH}}(t) = \frac{e}{\hbar} \sigma_{\text{SH}} E(t) \ell_D \left(\frac{1}{\sigma_m} - \frac{1}{\sigma_M} \right). \quad (15)$$

Here, σ_M and σ_m are the majority-spin and minority-spin conductivities, as mentioned above. Therefore, by measuring the electric voltage difference $V_{\text{SH}}(t)$, the spin Hall conductivity σ_{SH} can be determined.

V. SUMMARY

In summary, we have developed an analytical theory of the ac QSH effect by using the time-dependent scatter-

ing matrix method. The resulting ac spin current flowing from the QSH material into an electrode is linked to the winding numbers of the reflection matrix of the electrode, which also equal to the spin Chern numbers of the QSH system. The ac QSH effect is a bulk transport phenomenon, being substantially different from its dc counterpart, which relies on the existence of symmetry-protected gapless edge states. A possible way to observe the ac QSH effect experimentally was also suggested.

Acknowledgments

This work was supported by the State Key Program for Basic Researches of China under grants numbers 2015CB921202 and 2014CB921103 (L.S.), the National Natural Science Foundation of China under grant numbers 11674160 and 11225420 (L.S.), and a project funded by the PAPD of Jiangsu Higher Education Institutions (L.S. and D.Y.X.). This work was also supported by the U.S. Department of Energy, Office of Basic Energy Sciences under Grant No. DE-FG02-06ER46305 (D.N.S.).

-
- [1] C. L. Kane and E. J. Mele, Phys. Rev. Lett. **95**, 226801 (2005).
- [2] B. A. Bernevig and S. C. Zhang, Phys. Rev. Lett. **96**, 106802 (2006).
- [3] C. Wu, B. A. Bernevig, and S.-C. Zhang, Phys. Rev. Lett. **96**, 106401 (2006).
- [4] J. E. Moore and L. Balents, Phys. Rev. B **75**, 121306(R) (2007).
- [5] L. Fu and C. L. Kane, Phys. Rev. B **76**, 045302 (2007); L. Fu, C. L. Kane, and E. J. Mele, Phys. Rev. Lett. **98**, 106803 (2007).
- [6] H. J. Zhang, C. X. Liu, X. L. Qi, X. Dai, Z. Fang, and S. C. Zhang, Nature Phys. **5**, 438 (2009).
- [7] M. Z. Hasan and C. L. Kane, Rev. Mod. Phys. **82**, 3045 (2010).
- [8] X. L. Qi and S. C. Zhang, Physics Today. **63**, 33 (2010).
- [9] Y. Ando, J. Phys. Soc. Japan **82**, 102001 (2013).
- [10] J. E. Moore, Nat. Phys. **11**, 897 (2015).
- [11] H. Weng, R. Yu, X. Hu, X. Dai, and Z. Fang, Adv. Phys. **64**, 227 (2015).
- [12] B. A. Bernevig, Nat. Phys. **11**, 698 (2015).
- [13] Y. F. Ren, Z. H. Qiao, and Q. Niu, Rep. Prog. Phys. **79**, 066501 (2016).
- [14] C. L. Kane and E. J. Mele, Phys. Rev. Lett. **95**, 146802 (2005).
- [15] D. N. Sheng, Z. Y. Weng, L. Sheng, and F. D. M. Haldane, Phys. Rev. Lett. **97**, 036808 (2006).
- [16] E. Prodan, Phys. Rev. B **80**, 125327 (2009); E. Prodan, New J. Phys. **12**, 065003 (2010).
- [17] H. C. Li, L. Sheng, D. N. Sheng, and D. Y. Xing, Phys. Rev. B **82**, 165104 (2010).
- [18] Y. Yang, Z. Xu, L. Sheng, B. G. Wang, D. Y. Xing, and D. N. Sheng, Phys. Rev. Lett. **107**, 066602 (2011).
- [19] M. König, S. Wiedmann, C. Brüne, A. Roth, H. Buhmann, L. W. Molenkamp, X.-L. Qi, and S.-C. Zhang, Science **318**, 766 (2007).
- [20] I. Knez and R.-R. Du, Frontiers of Phys. **7**, 200 (2012).
- [21] W. Y. Deng, H. Geng, W. Luo, W. Chen, L. Sheng, D. N. Sheng, and D. Y. Xing, arXiv:1606.08301 (2016).
- [22] H. Jiao and G. E. W. Bauer, Phys. Rev. Lett. **110**, 217602 (2013).
- [23] D. Wei, M. Obstbaum, M. Ribow, C. H. Back, and G. Woltersdorf, Nat. Commun. **5**, 3768 (2014).
- [24] M. Büttiker, H. Thomas, and A. Prêtre, Z. Phys. B **94**, 133 (1994).
- [25] P. W. Brouwer, Phys. Rev. B, **58**, R10135 (1998).
- [26] B. A. Bernevig, T. L. Hughes, and S. C. Zhang, Science **314**, 1757 (2006).
- [27] C. X. Liu, T. L. Hughes, X. L. Qi, K. Wang, and S. C. Zhang, Phys. Rev. Lett. **100**, 236601 (2008).
- [28] H. Li, L. Sheng, R. Shen, L. B. Shao, B. Wang, D. N. Sheng, and D. Y. Xing, Phys. Rev. Lett. **110**, 266802 (2013).
- [29] M. N. Chen, L. Sheng, R. Shen, D. N. Sheng, and D. Y. Xing, Phys. Rev. B **91**, 125117 (2015).
- [30] S. Zhang, Phys. Rev. Lett. **85**, 393 (2000).
- [31] R. E. Camley and J. Barnaś, Phys. Rev. B **664**, 266802 (1989).
- [32] M. Liu and D. Y. Xing, Phys. Rev. B **47**, 12272 (1993).